Measurement of the ^{27}Al(n,α) and ^{27}Al(n,p) reaction cross section in the energy region 15.2 to 37.2 MeV

Muhammad Zaman [a], Guinyun Kim [a*], Kwangsoo Kim [a], Haladhara Naik[b], Sangil Park[a], Muhammad Shahid[a], Muhammad Nadeem[a]
[a]*Department of Physics, Kyungpook National University, Daegu 702-701, Republic of Korea*
[b]*Radichemistry Division, Bhaba Atomic Research Centre, Trombay, Mumbai-40085, India*
[*]*Corresponding author: gnkim@knu.ac.kr*

1. Introduction

The cross sections of the ^{27}Al(n,α)^{24}Na and ^{27}Al(n,p)^{27}Mg reactions were reported in Refs.[1]. These published data reveal that reactions cross section data of ^{27}Al(n,α)^{24}Na and ^{27}Al(n,p)^{27}Mg reactions at neutron energy above 20 MeV are rare and scanty. However, in the present work, we have measured for neutron energies of 15.2, 26.4 and 37.2 MeV to strengthen the data base. The shape of the cross sections well describes in both the evaluated libraries ENDF/B-VII.1 [2] and the theoretical data using the TALYS 1.6 code [3], but they differ in absolute values. In the present work, we determine the cross sections for the ^{27}Al(n,α)^{24}Na and ^{27}Al(n,p)^{27}Mg reactions in the neutron energy range from 15.2 to 37.2 MeV using an activation and off-line γ-ray spectrometric technique. The present measured values are compared with the data in both the EXFOR library [1], evaluated nuclear data library ENDF/B-VII.1 [2] and the TENDL-2013 library [4] based on the TALYS 1.6 code.

2. Experimental Details

The experiment was performed by using the quasi-mono energetic neutrons produced from a ^{9}Be(p,xn) reaction with 25, 35, and 45 MeV proton beam of the MC-50 cyclotron at the Korean Institute of Radiological and Medical Sciences (KIRAMS) [5-7]. The enriched ^{9}Be (purity ≤ 99%) metallic foil with a size of 25 mm × 25 mm was used for neutron production target. Behind a 2 mm thick B- target, a thick graphite plate was used to stop the lower energy proton beam. The thickness of graphite plate was 6 mm, 6 mm, and 12 mm for 25, 35, and 45 MeV proton beam. The 100 μm thick Au foil placed at 3.5 cm from the Be-target was used to monitor the neutron flux. We calculated the neutron spectra considering the Gaussian broadening with the MCNPX code [8]. The peak energy (E_p) and the FWHM values when the 45 MeV proton injected to the Be target are about 37.2 MeV and 4.40 MeV. Similarly, we got the peak energy E_p ~ 26.40 MeV and the FWHM ~ 5.54 MeV for the 35 MeV, and the E_p ~ 15.2 MeV and the FWHM ~ 7.30 MeV for the 25 MeV. The calculated spectra of these neutron fields are not purely mono-energetic but there are high energy distributions coming from the ^{9}Be(p,n) reaction and low energy tails from the consequent break-up reaction [9] as shown in Fig. 1.

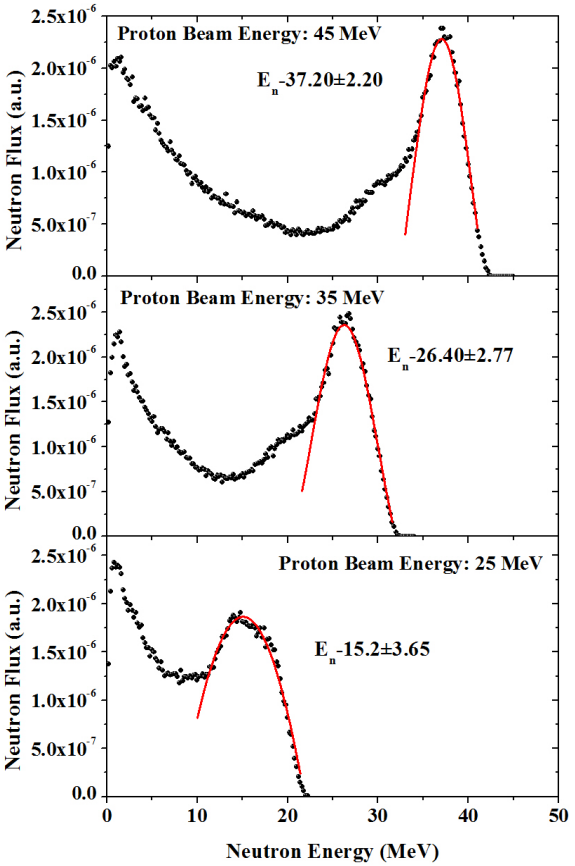

Fig. 1. Neutron spectra calculated using MCNPX for proton beam energies of 2, 35 and 45 MeV.

A 100-μm-thick ^{27}Al foil was used for irradiation. The sample assembly was positioned at 3.5 cm from the Be target and at zero degree with respect to the direction of the proton beam direction. The sample assembly was irradiated with high energy neutrons for 0.5 -1.0 h depends on the proton beam energy. Details of experimental conditions and sample characteristics are given in Table I.

Table I. Experimental conditions and characteristics of sample

Proton Beam Energy (MeV)	Irradiation Time (min)	Au-Mass (g)	Al-Mass (g)
25	60	0.296	0.090
35	60	0.219	0.065
45	30	0.244	0.097

The irradiated sample assembly was waited for 30 min to allow the decay of short-lived radioactive reaction products to avoid their radioactivity. Then Au and Al were taken out from the irradiated assembly and mounted on Perspex (acrylic glass, 1.5 mm thick) plate. The γ-ray counting of the reaction products from the ^{197}Au and ^{27}Al, samples was done by using an energy- and efficiency-calibrated HPGe detector coupled to a PC based 4 K-channel analyzer.

2. Data Analysis

2.1 Calculation of neutron flux

The numbers of observed γ-rays (N_{obs}) corresponding to the photo-peak was determined by summing the counts under the full energy peak and subtracting the linear Compton background. The neutron flux measurements are based on the activities of 355.68, 98.85, and 293.55 keV γ-rays of the ^{197}Au(n,2n), ^{197}Au(n,3n) and ^{197}Au(n,4n) reactions for 25, 35 and 45 MeV proton beam, respectively. The neutron flux (ϕ_n) is related to the known cross section (σ_R) of ^{197}Au(n,xn) reactions [10, 11] and the numbers of observed γ-rays (N_{obs}) under the photo-peak of an individual nuclide of interest as follows:

$$\phi_n = \frac{N_{obs}\left(T_{clock}/T_{count}\right)\lambda}{n\sigma_R I_\gamma \varepsilon\left(1-e^{-\lambda T_i}\right)e^{-\lambda T_c}\left(1-e^{-\lambda T_{count}}\right)} \quad (1)$$

where n is the number of target atoms, I_γ is the branching intensity of the analyzed γ-rays, ε the detection efficiency, λ (=$ln2/T_{1/2}$) is the decay constant for the isotope of interest, T_i, T_c, T_{clock}, and T_{count} are the irradiation time, the cooling time, the clock time and live time of counting, respectively. The nuclear spectroscopic data used for determining the neutron flux were given in Table II [12].

Table II. Nuclear spectroscopic data

Reaction	Half-life	Eγ-(keV)	Iγ-(%)	Decay mode
^{27}Al(n,α)^{24}Na	14.95 h	1368.6	100	β-(100)
^{27}Al(n,p)^{27}Mg	9.46 m	843.7	71.8	β-(100)
^{197}Au(n,2n)^{196}Au	6.18 d	355.68	87.0	EC(92.8) β$^-$(7.2)
^{197}Au(n,3n)^{195}Au	186.0 d	98.85	10.9	EC(100)
^{197}Au(n,4n)^{194}Au	38.02 h	293.55	10.4	EC(100)

The neutron spectra for the proton energies of 45, 35, and 25 MeV were calculated by using the MCNPX code and are shown in Fig. 1. The peak neutron energies in the neutron spectra for proton energies of 45, 35, and 25 MeV are 37.20±2.20, 26.40±2.77, and 15.20±3.65 MeV, respectively. The neutron fluxes ($\phi(E_n)$) at certain neutron energy were measured by using the ^{197}Au(n,2n), ^{197}Au(n,3n), and ^{197}Au(n,4n) reactions with known cross sections $\sigma_R(E_n)$ and Eq. (1)**.** The neutron fluxes will be measured from the reaction threshold to the maximum neutron energies.

The number of observed γ-ray (N_{obs}) under the characteristic gamma peaks from the ^{197}Au(n,2n), ^{197}Au(n,3n), and ^{197}Au(n,4n) reactions were related to the reaction cross section $\sigma_R(E_n)$ for the ^{197}Au(n,xn) reaction and the neutron flux. However, the measured neutron flux for the peak neutron energy region (peak neutron energy $E_p \pm \Delta E$~(FWHM/2) will be estimated by using the modified number of γ-ray (N_{obs}) in Eq. (1). In order to estimate the modified number of γ-ray in the peak neutron energy region, $M_{obs}=FACT\times N_{obs}$, we have to define a modification factor *FACT* as follows:

$$FACT = \int_{E_p-\Delta E}^{E_p+\Delta E}\sigma_R(E_n)\phi_n(E_n)dE_n \Big/ \int_{E_{th}}^{E_{max}}\sigma_R(E_n)\phi_n(E_n)dE_n \quad (2)$$

where $\phi(E_n)$ is the neutron flux calculated with the MCNPX code, E_{th} and E_{max} is the reaction threshold and the neutron end-point energy. E_p is the peak neutron energy and ΔE is the half of the FWHM from the Gaussian fitting as shown in Fig. 2.

This FACT calculated using Eq. (2) was used to modify the number of observed γ-ray (N_{obs}), when we estimated the neutron flux, i.e., $M_{obs}=FACT\times N_{obs}$, in Eq. (1). In order to calculate neutron fluxes for ^{27}Al(n,α)^{24}Na and ^{27}Al(n,p)^{27}Mg reactions in the peak neutron energy region $E_p\pm\Delta E$, we estimated the modified factor FACT for each nuclear reaction. The reaction cross section $\sigma_R(E_n)$ used in Eq. (2) for the ^{27}Al(n,α) and the ^{27}Al(n,p) reactions were taken from TENDL-2013 library.

2.2 Calculation of reaction cross section

In the present work, the radio-nuclides produced from the ^{27}Al(n,α) reaction was ^{24}Na and those from the ^{27}Al(n,p) reaction was ^{27}Mg. The net peak areas (N_{obs}) corresponding to the photo-peak for different reaction products were calculated by summing the counts under the peak neutron energy region and subtracting the linear Compton background. From the observed net photo-peak area (N_{obs}) of the produced nuclides, ^{24}Na from the ^{27}Al(n,α) reactions, ^{27}Mg from the ^{27}Al(n,p) reactions, we could determine the reaction cross sections in the peak neutron energy region using the following equation:

$$\sigma_R\left(E_P \pm \Delta E\right) = \frac{M_{obs}\left(T_{clock}/T_{count}\right)\lambda}{n\phi_n\left(E_P \pm \Delta E\right)I_\gamma \varepsilon\left(1-e^{-\lambda T_i}\right)e^{-\lambda T_c}\left(1-e^{-\lambda T_{count}}\right)} \quad (3)$$

where $M_{obs}=FACT\times N_{obs}$ and other parameters are the similar meanings in Eq. (1). The neutron fluxes

$\phi_n(E_p \pm \Delta E)$ measured in the peak neutron energy region were used to measure the reaction cross sections for the ^{27}Al(n,α) and the ^{27}Al(n,p) reactions.

3. Result and discussion

The radioactive nuclei ^{24}Na and ^{27}Mg, which were produced via the ^{27}Al(n,α)^{24}Na and ^{27}Al(n,p)^{27}Mg direct reactions beta decay to excited states of ^{24}Mg and ^{27}Al, respectively. These excited states then emitted γ-rays as the nuclei de-excite to their respective ground states. The γ-rays are detected and counted. From their numbers the neutron reaction cross sections are determined. In the present work, the cross sections for ^{27}Al(n,α)^{24}Na and ^{27}Al(n,p)^{27}Mg reactions were measured for the neutron energy range from 15.2 to 37.2 MeV and compared with earlier measurements and theoretically calculated values. Nuclear data from model calculations could potentially be used to validate the experimental data, if there is any lack of references data and/or shows any discrepancy among the various data sets in the literature. On the other hand, reliable experimental cross section data are necessary to probe and improve the results of model calculations. We compared the measured cross sections with ENDF/B-VII. and theoretical values of TENDL-2013 for the purpose of cross validation.

The ^{24}Na radio-nuclide is formed directly from the ^{27}Al(n,α)^{24}Na reactions with threshold energies 3.25 MeV and half-life ($T_{1/2}$ = 14.95 h) (Table II). The ^{24}Na beta decay feeds into the second excited state of ^{24}Mg (99.94%) of the time. Subsequently, the first excited state de-excites 100% of the time to the ground state, emitting a 1.368 MeV γ-ray making this transition a good indicator of the measure of activation of the aluminum sample.

Experimental results were obtained for the neutron energy of 15.2, 26.4 and 37.2 MeV for ^{27}Al(n,α)^{24}Na reaction. The present measured values were compared with model calculations (TENDL-2013), ENDF/B-VII. data and literature data [2]. The measured data agreed with the model calculations and literature data [1]. The present values are shown in Fig. 3 and given in Table IV. The measured data agreed with the model calculations and literature data. The present measured values are in good agreement with literature values, ENDF/B-VII. data and model calculations.

Table IV. the measured cross sections values for ^{27}Al(n,α) and ^{27}Al(n,p) reactions

E_n (MeV)	Reaction Cross section (mb)	
	^{27}Al(n,α)^{224}Na	^{27}Al(n,p)^{27}Mg
15.2±3.65	110.6±12.15	57.00±6.00
26.4±2.77	13.23±1.47	16.42±2.27
37.2±2.20	19.95±3.17	06.76±1.36

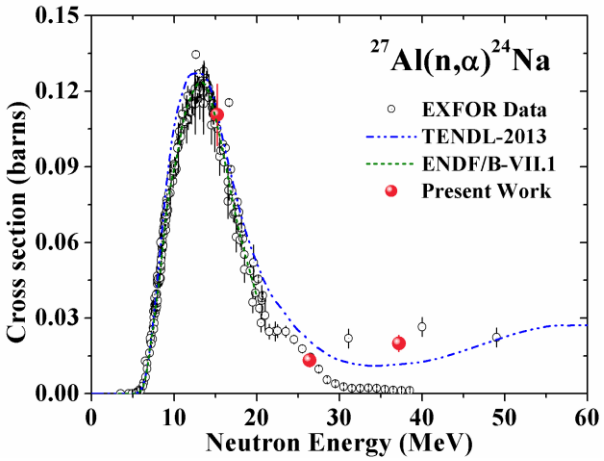

Fig.3. Experimental results for the neutron reaction cross sections of ^{27}Al(n,α)^{27}Mg reaction.

The ^{27}Mg nuclide is formed from the ^{27}Al(n,p)^{27}Mg reaction (E_{th} = 1.90 MeV) and half-life ($T_{1/2}$ = 9.46 min). The beta decay of ^{27}Mg feeds the first and second excited states of ^{27}Al. These states de-excite and emit 843.7 and 1014 keV γ-rays with branching fractions of 71.8 % and 28.2 %, respectively. Data were taken for different cooling times and average value was obtained. The present measured values for neutron energy of 15.2, 26.4 and 37.2 MeV are in good agreement with ENDF/B-VII. and literature data [1].

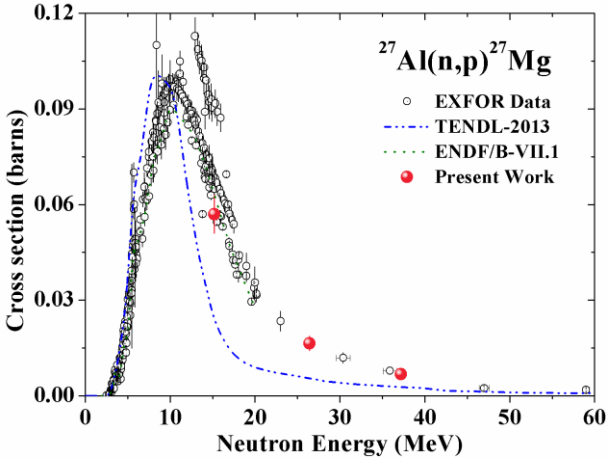

Fig.4. Experimental results for the neutron reaction cross sections of ^{27}Al(n,α)^{27}Mg reaction.

4. Uncertainty

We have measured ^{27}Al(n,α) and ^{27}Al(n,p) reaction cross sections for 15.2-37.2 MeV neutron beam. The uncertainties associated in measurement are based on the replicate measurements. The overall uncertainty is the quadratic sum of both statistical and systematic errors. The random error in the observed activity is due to counting statistics, which can be determined by accumulating the data for an optimum time period that depends on the half-life of the nuclide of interest. The systematic errors are due to uncertainties in the

irradiation time, the detection efficiency calibration, the uncertainty in the neutron flux, the half-life of nuclides of interest and the γ-ray abundance. In the determination of neutron flux at neutron peak energy, the contribution from the low-energy tail was subtracted by using TENDL-2013 cross section library and neutron flux profile estimated from MCNPX. Error of 5% was proposed by Honusek *et al.* for this procedure [13].

5. Conclusions

Neutron activation cross sections induced in ^{27}Al at 15.2, 26.4 and 37.2 MeV were measured by the activation and off-line gamma spectroscopy technique by using quasi-mono energetic neutron fields from the ^{9}Be(p,xn) reactions. Quasi-mono-energetic neutron sources from the ^{9}Be(p,xn) reaction for proton beam energies of 25, 35 and 45 MeV at KIRAMS were used. The present measured values were compared with theoretical model TENDL-2013, ENDF/B-VII. and with results from earlier measurements. The present results are in a good agreement with the experimental literature data. These experimental results will be useful as benchmark values to evaluate nuclear data and investigate the accuracy of calculation codes.

REFERENCES

[1] EXFOR (Experimental Nculear Reaction Data File). https://wwwnds.iaea.org/exfor/.
[2] Evaluated Nuclear Data File (ENDF), Database Version October 22, 2014. (https://www-nds.iaea.org/exfor/endf.htm).
[3] A. J. Koning, S. Hilaire and M. C. Duijvestijn, TALYS-1.6, A nuclear reaction program, NRG-1755 NG Petten, The Netherlands, 2008, http://www.talys.eu.
[4] A. J. Koning and D. Rochman, Nuclear Data Sheets, Vol. 113, p. 2841, 2012.
[5] M. Khandaker, A. Meaze, K. Kim, D. Son, G. Kim and Y. Lee, Journal of Korean Physical Society, Vol. 48, p. 821, 2006.
[6] M. Khandaker, M. Uddin, K. Kim, Y. Lee, G. Kim and Y. Lee, Nuclear Instruments and Methods in Physics Research Section B, Vol. 262, p. 171, 2007.
[7] M. Zaman, G. Kim, H. Naik, K. Kim and M. Shahid, Journal of Radioanalytical and Nuclear Chemistry, Vol. 303, p. 815, 2014.
[8] J. S. Hendricks, W. M. Gregg, L. F. Michael, R. J. Michael, C. J. Russell, W. D. Joe, P. F. Joshua, B. P. Denise, S. W. Laurie and W. M. William, MCNPX 2.6.0 Extensions, LANL Report LA-UR-08-2216, Los Alamos, URL http://mcnpx.lanl.gov/, 2008.
[9] H. Yashima, S. Sekimoto, T. Utsunomiya, K. Ninomiya, T. Omoto, R. Nakagaki, T. Shima, N. Takahashi, A. Shinohara and H. Matsumura, Proceedings in Radiochemistry A Supplement to Radiochimica Acta, Vol. 1, p. 135, 2011.
[10] Y. Uwamino, H. Sugita, Y. Kondo and T. Nakamura, Nuclear Data for Science and Technology, p. 726, 1992.
[11] B. Bayhurst, J. Gilmore, R. Prestwood, J. Wilhelmy, N. Jarmie, B. Erkkila and R. Hardekopf, Physical Review C, Vol. 12, p. 451, 1975.
[12] R. B. Firestone and L. P. Ekström, WWW Table of Radioactive Isotopes, Ver. 2.1, URL http://ie.lbl.gov/toi/, 1999.
[13] M. Honusek, P. Bém, U. Fischer, M. Götz, J. Novák, S. Simakov and E. Šimečková, Journal of Korean Physical Society, Vol. 59, p. 1374, 2010.